*Preprint* — This manuscript has been submitted to *Minerals Engineering* (Elsevier) and is currently under peer review.

# Coupling Chemistry and Machine Learning Across the Lithium Supply Chain: Resource Geochemistry, Extraction, Separation, and Recycling

Mustafa Rezaei[1,*], Gabriela Sanchez-Lecuona[2], and Omid Abdolazimi[3]

[1] Department of Computer Science, Boise State University, 1910 University Drive, Boise, ID 83725, USA

[2] Department of Chemistry, Mississippi State University, Hood Drive, Mississippi State, MS 39762, USA

[3] Department of Industrial and Systems Engineering, Mississippi State University, Hood Drive, Mississippi State, MS 39762, USA

* Corresponding author: mustafarezaei@u.boisestate.edu

**Submission details**

Journal: Minerals Engineering (Elsevier); ISSN 0892-6875

Article type: Review article

Current status: Under review

**Suggested citation**

Rezaei, M., Sanchez-Lecuona, G., Abdolazimi, O., 2026. Coupling chemistry and machine learning across the lithium supply chain: resource geochemistry, extraction, separation, and recycling. Preprint, submitted to *Minerals Engineering*. SSRN.

**Coupling Chemistry and Machine Learning Across the Lithium Supply Chain: Resource Geochemistry, Extraction, Separation, and Recycling**

Mustafa Rezaei [1,*], Gabriela Sanchez-Lecuona [2], and Omid Abdolazimi [3]

1 Department of Computer Science, Boise State University, 1910 University Drive, Boise, ID 83725, USA; mustafarezaei@u.boisestate.edu

2 Department of Chemistry, Mississippi State University, Hood Drive, Mississippi State, MS 39762, USA; gs1049@msstate.edu

3 Department of Industrial and Systems Engineering, Mississippi State University, Hood Drive, Mississippi State, MS 39762, USA; oa220@msstate.edu

## Abstract

Lithium supply must expand sharply over the coming decades to support the electrification of transport and the growth of stationary energy storage. At almost every stage the governing chemical challenge is the same: concentrating and separating $Li^+$ from chemically similar competing ions at acceptable economic and environmental cost. This review examines the supply chain through two interconnected lenses the chemical mechanisms that govern lithium recovery, and the data-driven methods used to characterize resources, model processes, and optimize recovery. We first summarize the geochemistry that controls where lithium concentrates, from lithium-cesium-tantalum pegmatites and closed-basin brines to volcano-sedimentary claystones and oilfield waters, and show how machine-learning resource assessment has revised occurrence estimates, notably for the Smackover Formation of Arkansas. We then review the chemistry of the three primary recovery routes spodumene conversion and acid roasting, evaporative brine processing, and direct lithium extraction by aluminate sorbents, ion sieves, membranes, and electrochemical systems together with the purification steps that turn concentrates into battery-grade chemicals, where magnesium and calcium removal dominates refining cost. Recycling is treated as an emerging fourth resource: pyrometallurgical, hydrometallurgical, early-stage selective, and direct-regeneration routes are compared against the recovery targets of the European Union battery regulation. Throughout, we assess where machine learning, surrogate modeling, and process optimization have delivered validated gains from sorbent design to battery sorting and where claims outrun evidence. We close with an integrated framework linking chemical mechanism to data-driven development, and identify data scarcity, absent benchmarks, and limited transferability as the binding constraints of the next decade.

**Keywords:** lithium; direct lithium extraction; hydrometallurgy; battery recycling; machine learning; process optimization

## 1. Introduction

The scale of the lithium market has changed faster than almost any other segment of the mineral industry. World mine production (excluding the United States) reached approximately 290,000 t of lithium in 2025, up from about 204,000 t in 2023, with Australia, China, Chile, Zimbabwe, and Argentina as the leading producers; batteries now account for 88% of end use (USGS, 2026). Identified resources have been revised upward repeatedly to roughly 150 Mt of contained lithium at the latest count, against reserves of 37 Mt (USGS, 2026) a striking contrast with assessments from little more than a decade ago,

when global resources were estimated near 31 Mt and long-term adequacy was an open question (Kesler et al., 2012). Demand has kept pace: the International Energy Agency reports that lithium demand grew by nearly 30% in 2024 alone and projects a fivefold increase by 2040 under stated policies, with announced mining projects implying a supply shortfall on the order of 40% by 2035 (IEA, 2025). Prices have amplified these signals rather than smoothing them. The annual average United States fixed-contract price of battery-grade lithium carbonate rose from roughly US$12,000–14,000 per tonne in 2021 to more than US$60,000 in 2022, then collapsed by over 80% to about US$9,000 by 2025 (USGS, 2026; IEA, 2025). Volatility of this magnitude complicates project financing across a sector in which new mines routinely take a decade to permit and build, and it strengthens the case for supply routes brine processing intensification, unconventional resources, and recycling that can respond to demand on shorter timescales. Fig. 1 summarizes the current production and resource landscape.

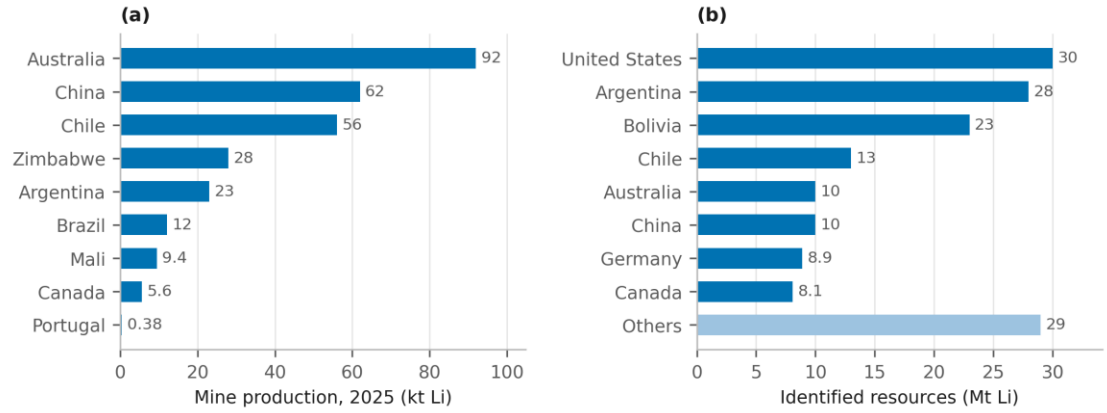


**Fig. 1.** The global lithium supply landscape. (a) Mine production in 2025 by country (United States production withheld in the source). (b) Identified lithium resources by country; “Others” aggregates the remaining countries in the source list. Data from USGS (2026).

Beneath the market numbers lies a chemical problem that is easy to state and hard to solve. Lithium is not geochemically scarce; the upper continental crust contains on the order of 24–35 ppm (Rudnick and Gao, 2003; Teng et al., 2004). But the same properties that make lithium valuable in batteries small ionic radius, low mass, high charge density make it difficult to concentrate and to separate. In magmatic systems lithium behaves incompatibly and accumulates only in extremely fractionated residual melts; in aqueous systems it is highly soluble, resists precipitation as an evaporite mineral, and travels with sodium, potassium, and especially magnesium, whose ionic radius in six-fold coordination (72 pm) is nearly identical to that of lithium (76 pm). Nearly every technical bottleneck reviewed in this paper the energy demanded by spodumene conversion, the slow attrition of lithium in evaporation ponds, the magnesium-to-lithium ratio that disqualifies otherwise attractive brines, the cost of removing magnesium and calcium from crude carbonate, the loss of lithium to slag in battery smelting is a manifestation of this selectivity problem. Framing the supply chain around selectivity, rather than around deposit inventories, is the first organizing choice of this review.

The second is to treat data-driven methods as part of the supply chain rather than as an appendix to it. Over the past five years, machine learning has moved from a speculative theme in lithium research to a set of working tools with documented results. A random-forest model trained on historical brine analyses underpins the United States Geological Survey's assessment of 5.1–19 Mt of lithium in Smackover Formation brines of southern Arkansas a single study that materially changed the national resource outlook (Knierim et al., 2024). Artificial neural networks and support vector machines applied to satellite imagery and geochemistry have mapped prospective lithium pegmatites in Iberia (Cardoso-Fernandes et al., 2020a; Köhler et al., 2021). Interpretable machine learning has guided the design of doped aluminum-based sorbents for salt-lake brines that were then synthesized and validated experimentally (Zhang et al., 2025), and gradient-boosting models predict lithium uptake on ion sieves across heterogeneous water chemistries with high fidelity (Xu et al., 2024). In recycling, federated learning has been used to sort retired batteries by cathode chemistry from a single diagnostic cycle (Tao et al., 2023), and computer vision guides robotic disassembly of battery packs (Zorn et al., 2022). These are no longer proposals; they are results, and a review of lithium recovery that ignores them describes a field that no longer exists. At the same time, the literature contains claims that outrun evidence digital twins of evaporation ponds, autonomous process control of direct lithium extraction and part of our purpose is to separate the demonstrated from the aspirational.

Several excellent reviews cover parts of this territory: lithium resource availability and extraction innovation (Tabelin et al., 2021), brine processing and its environmental footprint (Flexer et al., 2018; Vera et al., 2023), lithium recovery materials (Xu et al., 2016; Xu et al., 2021), battery recycling (Harper et al., 2019; Neumann et al., 2022; Biswal et al., 2024), and machine learning in battery end-of-life management (Tao et al., 2026). What is missing, in our reading, is an integrated treatment that follows the chemistry of the lithium ion from source rock to battery-grade salt to recycled black mass, and that evaluates critically and with verified examples where data-driven methods have genuinely accelerated each stage. That integration reflects the composition of our team, which spans geosciences, chemistry, and industrial and systems engineering, and it defines the contribution we intend here. We have previously applied a similar cross-disciplinary structure to the rare earth elements (Rezaei et al., 2025).

The review is organized as follows. Section 2 establishes the geochemical framework: where lithium concentrates, in what phases, and at what grades, ending with the data-driven assessment methods now reshaping resource inventories. Section 3 reviews the extraction chemistry of the three primary routes hard-rock processing, evaporative brine concentration, and direct lithium extraction and the computational and statistical tools used to design and optimize them. Section 4 addresses the purification chemistry that converts concentrates into battery-grade lithium carbonate and hydroxide. Section 5 treats recycling as an emerging fourth resource stream, comparing process routes against regulatory recovery targets and reviewing the role of machine learning in sorting, triage, and disassembly. Section 6 compares the environmental performance of the supply routes on a life-cycle basis. Section 7 synthesizes the preceding sections into a framework linking

chemical mechanism to data-driven development and identifies the constraints most likely to bind over the next decade, and Section 8 concludes.

## 2. Geochemical framework of lithium resources

### 2.1 Crustal behavior and mineral hosts

Lithium's geochemical behavior follows directly from its position in the periodic table. As the smallest alkali metal, $Li^+$ substitutes readily for $Mg^{2+}$ and, to a lesser extent, $Fe^{2+}$ and $Al^{3+}$ in octahedral sites of ferromagnesian silicates, which is why ordinary micas and clays carry tens to hundreds of ppm of lithium without ever forming an ore. Concentration to economic levels requires either extreme magmatic fractionation, which excludes lithium from crystallizing phases until it saturates late-stage melts and fluids, or prolonged low-temperature aqueous cycling, which leaches lithium from volcanic glass and immature sediments and accumulates it in closed hydrologic systems. These two pathways produce the two great families of lithium deposits solid-hosted and brine-hosted whose contrasting chemistry dictates nearly everything about how they are mined and processed (Bradley et al., 2017; Bowell et al., 2020; Munk et al., 2016).

In solid-hosted deposits, the principal ore mineral is spodumene ($LiAlSi_2O_6$), a clinopyroxene containing a theoretical 3.7 wt% Li (8.0 wt% $Li_2O$), accompanied in various deposits by petalite ($LiAlSi_4O_{10}$), lepidolite ($K(Li,Al)_3(Al,Si)_4O_{10}(F,OH)_2$), and the phosphate amblygonite-montebrasite. Typical run-of-mine grades in lithium-cesium-tantalum (LCT) pegmatites are 1–2 wt% $Li_2O$, rising to about 2 wt% $Li_2O$ in reserves at Greenbushes in Western Australia, the largest hard-rock operation (Bowell et al., 2020). In volcano-sedimentary systems, lithium resides in smectitic and illitic clays at grades an order of magnitude lower typically 0.2–0.9 wt% Li but in laterally extensive, flat-lying bodies amenable to bulk mining (Castor and Henry, 2020; Benson et al., 2023). In brines, lithium is simply a dissolved trace constituent, ranging from 0.17 mg/L in seawater (Dugamin et al., 2021) through tens to hundreds of mg/L in geothermal and oilfield waters, to a mean of about 1,400 mg/L (locally up to 7,000 mg/L) in the Salar de Atacama, the highest-grade brine system known (Munk et al., 2016). Table 1 summarizes the principal resource classes, their lithium hosts, representative grades, and the extraction routes they feed, and Fig. 2 places their concentration ranges on a common logarithmic scale.

**Table 1.**
Principal lithium resource classes, their lithium hosts, representative grades or concentrations, and the extraction routes they feed. Compiled from Munk et al. (2016), Bradley et al. (2017), Bowell et al. (2020), Castor and Henry (2020), Dugamin et al. (2021), Stringfellow and Dobson (2021), Sanjuan et al. (2022), Benson et al. (2023), Knierim et al. (2024), and Harper et al. (2019).

| Resource class | Representative | Principal Li host | Typical grade / | Primary recovery route |
|---|---|---|---|---|

| | examples | | concentration | |
|---|---|---|---|---|
| LCT pegmatite | Greenbushes, Pilgangoora (Australia); Tanco (Canada); Jiajika (China) | Spodumene, petalite, lepidolite | 1–2 wt% $Li_2O$ ore; ~2 wt% $Li_2O$ reserves at Greenbushes | Concentration, calcination, acid roast (Section 3.1) |
| Closed-basin brine | Atacama, Hombre Muerto, Uyuni (Lithium Triangle); Qinghai–Tibet lakes (China) | Dissolved $Li^+$ | ~100–1,500 mg/L; Atacama mean ≈1,400 mg/L | Solar evaporation and precipitation; DLE (Sections 3.2–3.3) |
| Volcano-sedimentary claystone | Thacker Pass / McDermitt caldera (USA); Sonora (Mexico) | Smectite, illite | ~0.2–0.6 wt% Li | Acid or salt-roast leaching (under development) |
| Jadarite borosilicate | Jadar (Serbia) | Jadarite, $LiNaSiB_3O_7(OH)$ | ~1.8 wt% $Li_2O$ with ~13 wt% $B_2O_3$ | Hydrometallurgical (under development) |
| Geothermal brine | Salton Sea (USA); Upper Rhine Graben (France/Germany) | Dissolved $Li^+$ | ~150–440 mg/L | DLE only |
| Oilfield / basinal brine | Smackover Formation (USA) | Dissolved $Li^+$ | Mostly 0.5–37 mg/L; >400 mg/L locally in the Smackover | DLE only |
| Spent lithium-ion batteries | Global EV and electronics waste streams | Cathode oxides in black mass | Several wt% Li, cathode-dependent | Recycling routes (Section 5) |

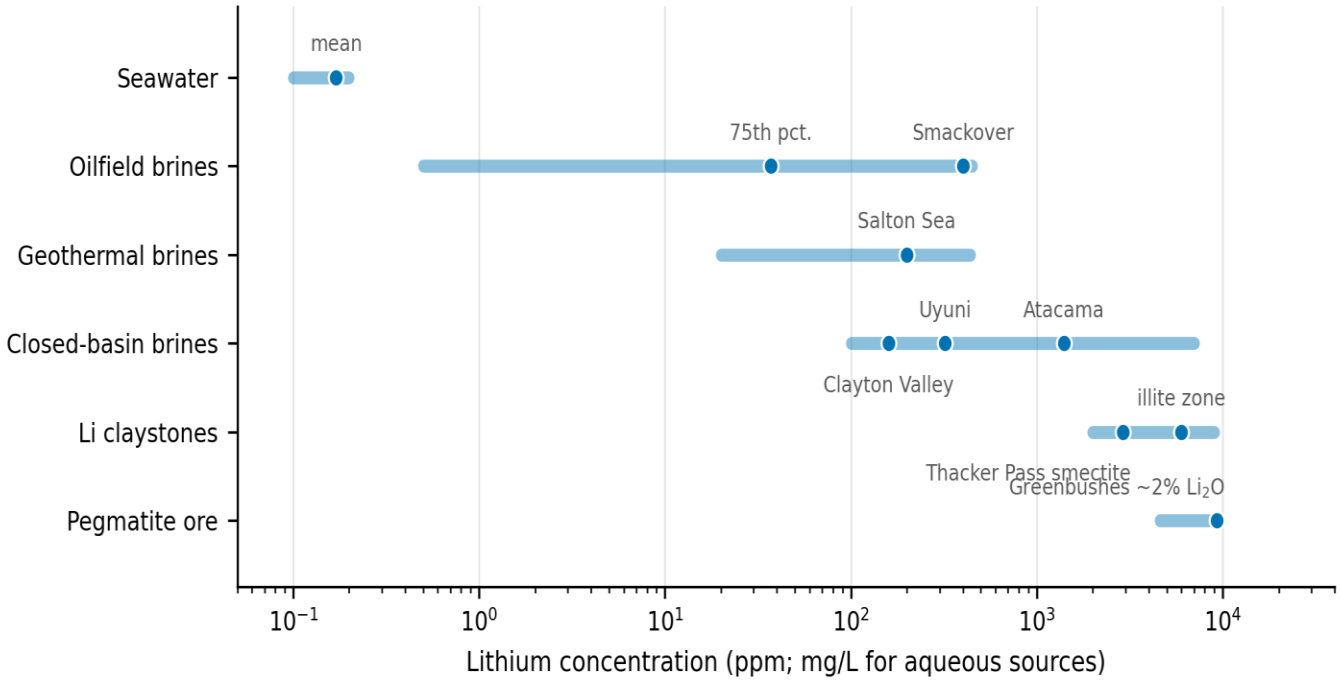

**Fig. 2.** Lithium concentration ranges across natural resource classes on a logarithmic scale, with representative deposits marked. Aqueous concentrations in mg/L; solid grades in ppm Li (2 wt% $Li_2O$ ≈ 9,300 ppm Li). Data from Munk et al. (2016), Dugamin et al. (2021), Stringfellow and Dobson (2021), Castor and Henry (2020), Benson et al. (2023), Bowell et al. (2020), and Knierim et al. (2024).

### 2.2 Deposit classes and their process-relevant chemistry

**LCT pegmatites.** Lithium-cesium-tantalum pegmatites are highly fractionated granitic dikes emplaced during the late stages of orogenic magmatism, internally zoned, with lithium minerals concentrated in intermediate and core zones (Bradley et al., 2017). From a processing standpoint their defining features are high grade, coarse crystal size permitting dense-media and flotation concentration to 5–6 wt% $Li_2O$, and a refractory host phase: α-spodumene is essentially inert to acid attack, which forces the energy-intensive thermal conversion described in Section 3.1. Major producing districts include Greenbushes and the Pilgangoora–Wodgina belt in Western Australia, the Tanco pegmatite in Canada, and the Jiajika field in China (Kesler et al., 2012; Bradley et al., 2017). Pegmatites currently supply more than half of world production despite hosting a modest share of world resources a mismatch explained by short development timelines and conventional flowsheets rather than by geology (USGS, 2026).

**Closed-basin brines.** Continental brines form where lithium leached from volcanic and crystalline rocks accumulates in endorheic basins under arid climates, concentrated by evaporation over geologic time. Because lithium salts are among the most soluble in the evaporite sequence, lithium remains in residual pore brines beneath salt crusts while halite, gypsum, and carbonates precipitate a natural pre-concentration that human operators extend in engineered ponds. The Lithium Triangle of Chile, Argentina, and Bolivia hosts the largest and richest examples, including the Salar de Atacama, Salar del Hombre Muerto, and Salar de Uyuni; comparable systems occur on the Qinghai–Tibet Plateau of China (Munk et al., 2016; López Steinmetz and Salvi, 2021). Two chemical parameters dominate brine economics: the absolute lithium concentration, and the Mg/Li mass ratio, which ranges from about 6 at Atacama to more than 60 in some Chinese salt lakes and controls reagent consumption in magnesium removal (Flexer et al., 2018; Vera et al., 2023). Basin size itself is a first-order control on brine grade in Andean salars (López Steinmetz and Salvi, 2021).

**Volcano-sedimentary claystones.** In caldera-hosted lacustrine basins, lithium leached from rhyolitic glass is fixed in neoformed clays. The McDermitt caldera of Nevada–Oregon is the type example: smectitic claystones averaging roughly 0.3 wt% Li are overprinted, in the Thacker Pass area, by an illitic zone carrying up to about 0.6 wt% Li formed by hydrothermal enrichment (Castor and Henry, 2020; Benson et al., 2023; Emproto et al., 2025). Peer-reviewed estimates place more than 1.5 Mt of contained lithium at Thacker Pass alone and 20–40 Mt across the caldera's claystones, which would rank the district among the largest known lithium accumulations of any type (Castor and Henry, 2020; Benson et al., 2023). The jadarite deposit at Jadar, Serbia where lithium is hosted in the borosilicate jadarite, $LiNaSiB_3O_7(OH)$ (Stanley et al., 2007) represents a chemically distinct variant with co-product boron. Claystone and jadarite ores are chemically reactive relative

to spodumene, and their processing challenges lie less in liberation than in reagent consumption by gangue carbonates and in generating large volumes of leached residue.

**Geothermal and oilfield brines.** Deep basinal and geothermal fluids acquire lithium through prolonged high-temperature water–rock interaction. Lithium-rich geothermal systems include the Salton Sea field in California, where post-flash brines average about 200 mg/L Li and could in principle supply 6,000–32,000 t of lithium per year at existing flow rates (Stringfellow and Dobson, 2021), and European systems of the Upper Rhine Graben with 150–200 mg/L (Sanjuan et al., 2022). Oilfield produced waters worldwide mostly carry 0.5–37 mg/L Li, but favorable formations reach far higher values (Dugamin et al., 2021); the Smackover Formation of the Gulf Coast, a Jurassic carbonate aquifer long exploited for bromine, locally exceeds 400 mg/L (Knierim et al., 2024). These resources are attractive because the fluid is already at surface pumped for power generation or hydrocarbon production so lithium recovery piggybacks on existing infrastructure. They are also the resources for which evaporative concentration is least feasible, because the fluids are dilute, hot, and reinjected; they therefore depend entirely on the direct extraction technologies of Section 3.3.

### 2.3 Data-driven resource assessment

Resource assessment has historically relied on deposit models and expert judgment. What has changed is the availability of large geochemical databases and the demonstration that supervised learning can interpolate sparse, biased legacy data well enough to support quantitative resource estimates.

The clearest case is the Smackover Formation. Knierim et al. (2024) trained a random-forest model on historical brine analyses from the USGS produced-waters database, using geologic, geochemical, and temperature predictors, to map lithium concentrations across southern Arkansas where sampling is uneven. Integrating the predicted concentration surface with aquifer geometry yielded 5.1–19 Mt of dissolved lithium in place 35–136% of the then-current national resource estimate and showed that roughly 5,000 t of lithium passed unrecovered through bromine-plant waste streams in 2022 alone. The result did not create the resource, but it converted an anecdote (“Smackover brines are lithium-rich”) into a mapped, uncertainty-bounded inventory that companies are now drilling against. Related work has benchmarked gradient-boosted trees and deep neural networks for predicting lithium in produced waters from routine major-ion analyses data that exist for hundreds of thousands of legacy wells including tests of transferability between basins (Attanasi et al., 2024, 2026). The practical significance is that the feature set (Cl, Br, Mg, K, Sr concentrations, temperature, depth) is exactly what historical records contain, so the models monetize data that already exist.

For solid-hosted resources, the analogous development is prospectivity mapping with remotely sensed and geochemical inputs. Support vector machines applied to Sentinel-2 imagery detected known lithium pegmatites in the Fregeneda–Almendra district of Iberia while controlling the overfitting that plagues small training sets (Cardoso-Fernandes et al., 2020a), and artificial neural networks combining geology, stream-sediment geochemistry, and satellite data mapped lithium potential over 1,200 $km^2$ of central Portugal, recovering

the known Bajoca and Feli deposits while suppressing false positives (Köhler et al., 2021). A caution belongs here: lithium itself has no diagnostic spectral absorption accessible from satellite platforms, so these methods detect proxies micas, alteration, morphology and inherit the ambiguity of proxies (Cardoso-Fernandes et al., 2020b). Claims of direct spectral detection of lithium from orbit should be read skeptically. At continental scale, gradient-boosting prospectivity models for sediment-hosted mineral systems have reduced search areas by more than 90% relative to conventional weights-of-evidence approaches (Lawley et al., 2022), a methodological template now being extended to lithium systems.

Field-portable spectroscopy closes the loop between prediction and verification. Laser-induced breakdown spectroscopy (LIBS) one of the few field techniques that measures light elements directly quantifies lithium in crushed pegmatite ore with calibration accuracies of $R^2 \approx 0.98$ against ICP-AES and simultaneously maps the ore mineralogy (Rifai et al., 2022), and handheld LIBS soil surveys have located a spodumene dike buried under 15 m of saprolite in the Carolina Tin-Spodumene Belt from the lithium anomaly in overlying soils (Harmon et al., 2025). Together, database-trained regional models, proxy-based remote sensing, and direct field measurement form a workflow in which each layer generates training data for the next structure we return to in Section 7.

## 3. Extraction chemistry of primary lithium

The three primary routes to lithium chemicals differ so much in their unit operations that they are best understood as three different chemistries aimed at the same product (Fig. 3). Hard-rock processing is high-temperature solid-state and acid-digestion chemistry; evaporative processing is fractional crystallization at ambient temperature over months; direct lithium extraction is interfacial coordination chemistry engineered into sorbents, membranes, and electrodes.

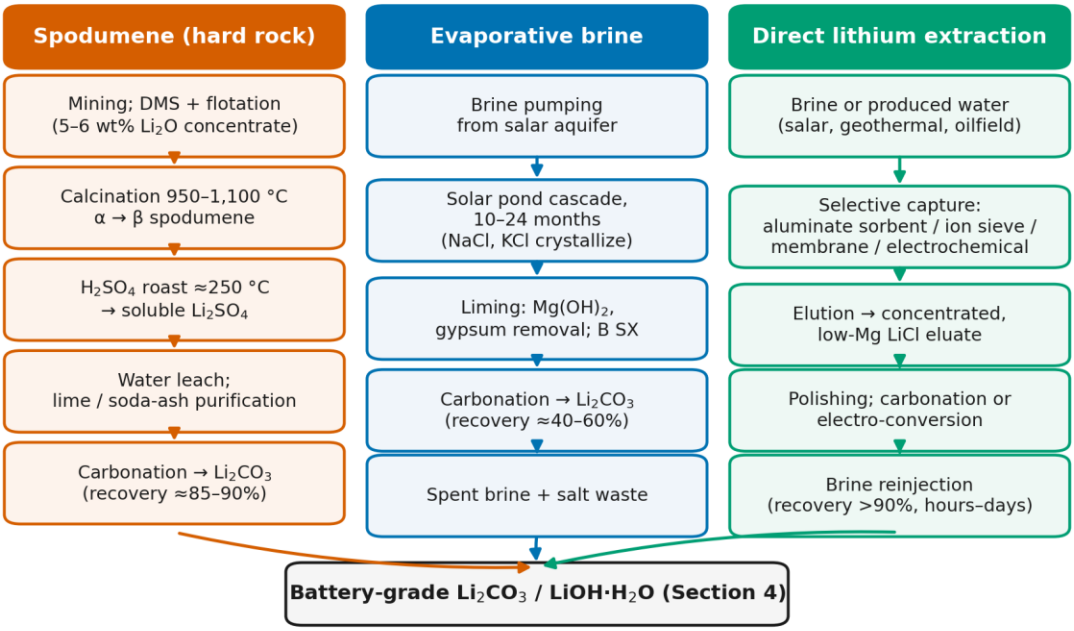

**Fig. 3.** Simplified flowsheets of the three primary lithium recovery routes, with characteristic conditions, timescales, and recoveries. Compiled from Dessemond et al. (2019), Meshram et al. (2014), Flexer et al. (2018), and Vera et al. (2023). DMS, dense-media separation; SX, solvent extraction.

### 3.1 The spodumene route

Natural α-spodumene is, for practical purposes, chemically inert: its dense monoclinic structure locks lithium into sites that neither hot concentrated acids nor bases reach at useful rates. Commercial practice therefore begins by destroying that structure. podumene concentrate (typically 5–6 wt% $Li_2O$ after dense-media separation and lotation) is calcined at 950–1,100 °C, where α-spodumene transforms to the open tetragonal β-polymorph ccompanied by a volume expansion and decrepitation that renders the mineral reactive (Salakjani et al., 2016; Dessemond et al., 2019). The transformation begins near 950 °C and is complete within minutes above about 1,050 °C; because it is reconstructive, it cannot be shortcut at lower temperature without prohibitively long residence times (Salakjani et al., 2016; Salakjani et al., 2020). The β-spodumene is then mixed with excess concentrated sulfuric acid and roasted at about 250 °C, where $H^+$ exchanges quantitatively for $Li^+$ to form water-soluble $Li_2SO_4$ while the aluminosilicate framework is left behind (Dessemond et al., 2019). Water leaching, impurity precipitation with lime and soda ash, and carbonation with $Na_2CO_3$ then yield technical-grade lithium carbonate; overall lithium recoveries of 85–90% are typical of well-operated plants (Meshram et al., 2014; Dessemond et al., 2019).

Two features of this flowsheet shape its economics and its environmental profile. The first is energy: the calcination and acid-roast steps make the ore route roughly seven times more energy-intensive than brine processing per tonne of lithium carbonate about 218,000 MJ/t against 30,000–36,000 MJ/t (Kelly et al., 2021). The second is the byproduct burden: nearly ten tonnes of aluminosilicate residue and sodium sulfate accumulate per tonne of carbonate, and the industry has yet to establish large-scale uses for either. Alternatives to the acid roast alkaline digestion, carbonate pressure leaching, chlorination roasting, and mechanochemical activation have each demonstrated high extractions at laboratory scale and are reviewed comprehensively elsewhere (Meshram et al., 2014; Karrech et al., 2020); none has displaced sulfuric acid at commercial scale, largely because the acid route's robustness to feed variability outweighs its reagent cost. Lepidolite and zinnwaldite ores, processed mainly in China, follow analogous roast–leach chemistry complicated by fluorine management (Choubey et al., 2016).

### 3.2 Evaporative processing of continental brines

The conventional brine flowsheet is fractional crystallization executed by the sun. Brine pumped from beneath the salar crust is transferred through a cascade of ponds where halite, sylvite, and carnallite crystallize sequentially as evaporation proceeds; over 10–24 months the lithium concentration rises from a few hundred mg/L to several percent (Flexer et al., 2018; Vera et al., 2023). Magnesium the critical impurity is removed by liming, which precipitate es $Mg(OH)_2$ and gypsum; boron is stripped by solvent extraction or acidification; and the concentrated liquor is finally carbonated to precipitate $Li_2CO_3$, exploiting the retrograde solubility of lithium carbonate in hot water (Flexer et al., 2018).

The chemistry is simple, the reagents cheap, and the energy demand low. The costs are time and yield: more than 90% of the salts crystallized in the ponds are waste, an appreciable fraction of the lithium is entrained in discarded salts or lost to pond leakage, and overall recoveries are commonly reported around 40–60% (Vera et al., 2023). The Mg/Li ratio determines where the flowsheet is viable at all: every unit of magnesium consumes lime stoichiometrically and generates sludge that traps lithium, which is why Atacama (Mg/Li ≈ 6) supports profitable operations while chemically similar but magnesium-rich brines do not (Flexer et al., 2018).

The deeper limitation is inflexibility. A pond system sized during construction cannot respond to the price swings described in Section 1, and its multi-month residence time makes process control an exercise in weather forecasting. These limitations, as much as the environmental concerns discussed in Section 6, explain the industrial momentum behind direct extraction.

### 3.3 Direct lithium extraction

Direct lithium extraction (DLE) designates any process that selectively removes lithium from a brine without evaporative pre-concentration, returning the spent brine to the basin or reservoir. Four chemical families dominate (Table 2).

**Aluminate sorbents.** Layered lithium–aluminum double hydroxides, $LiCl{\cdot}2Al(OH)_3{\cdot}nH_2O$, capture LiCl into vacant octahedral sites within gibbsite-like layers; the small size selectivity of these sites excludes $Na^+$, $K^+$, and hydrated $Mg^{2+}$, and lithium is released simply by washing with dilute water (Paranthaman et al., 2017; Xu et al., 2021). Capacities are modest on the order of 7–8 mg Li/g but selectivity, mild regeneration, and mechanical robustness have made aluminate sorbents the only DLE chemistry with long industrial history: they have operated at Salar del Hombre Muerto since the late 1990s, underpin adsorption plants on magnesium-rich Qinghai brines where evaporative processing is chemically foreclosed, and were selected for the plant commissioned at Centenario-Ratones, Argentina, in 2024 (Vera et al., 2023; Boroumand and Razmjou, 2024; Eramet, 2024).

**Ion-sieve oxides.** Spinel lithium manganese oxides, delithiated to protonated forms such as $H_{1.6}Mn_{1.6}O_4$, and layered titanates such as $H_2TiO_3$ act as true ion sieves: the $Li^+$ vacancies left by acid delithiation admit only ions of lithium's size. Theoretical capacities reach 72 mg/g for the manganese spinel, with 30–40 mg/g realized from natural brines and seawater, and about 33 mg/g for $H_2TiO_3$ from salt-lake brine at pH 6.5 (Chitrakar et al., 2001; Chitrakar et al., 2014; Xu et al., 2016). Their unresolved weakness is chemical: regeneration requires acid elution, and each acid cycle dissolves a fraction of the manganese framework through the disproportionation of $Mn^{3+}$, degrading capacity over the hundreds of cycles an industrial sorbent must survive (Xu et al., 2016). Titanium sieves resist dissolution better but bind lithium so strongly that elution kinetics suffer. Framework stabilization through doping, coatings, and binder engineering remains the central materials problem, and is the entry point for the machine-learning work described in Section 3.4.

**Solvent extraction and membranes.** Tributyl phosphate with $FeCl_4^-$ as a co-anion extracts LiCl from magnesium-rich brines with useful selectivity (Zhou et al., 2012), though solvent losses and equipment corrosion have confined the chemistry to niche deployment. Membrane processes approach the Mg/Li problem from charge and size: monovalent-selective nanofiltration membranes, typically polyamides bearing positive surface charge to repel divalent cations, achieve high Mg/Li separation factors and are extensively studied for magnesium-rich Chinese brines (Xu et al., 2021; Vera et al., 2023). Electromembrane and electrodialysis variants add an electric driving force at corresponding energy cost (Vera et al., 2023).

**Electrochemical intercalation.** Battery-electrode materials can be run in reverse as lithium pumps: a $LiFePO_4/FePO_4$ couple intercalates $Li^+$ selectively from brine at one electrode while releasing it into a clean recovery solution at the other, with selectivity inherited from the olivine lattice and energy consumption in principle limited to the small potential difference between the two solutions (Pasta et al., 2012; Battistel et al., 2020). Electrochemical systems are the least mature family but the most interesting thermodynamically, because they couple naturally to intermittent renewable power and avoid reagent cycles altogether.

Across families, reported single-pass recoveries above 90% and Li/Mg selectivities above 100 contrast with evaporative recoveries near 50% (Vera et al., 2023). The caveats deserve equal emphasis. DLE plants process enormous volumes of brine per tonne of product, consume fresh water for washing and elution a serious constraint in the same deserts whose water balance motivates DLE in the first place and must manage the thermal and chemical excursions of real brines rather than synthetic test solutions (Vera et al., 2023). Techno-economic analysis of geothermal DLE at the Salton Sea reaches guardedly positive conclusions but stresses the sensitivity of margins to sorbent lifetime, exactly the parameter least constrained by short laboratory campaigns (Warren, 2021; Stringfellow and Dobson, 2021).

**Table 2.** Direct lithium extraction technology classes: chemistry, performance, and status.

| Class | Working chemistry | Representative capacity | Strengths | Principal limitation | Status | Key sources |
|---|---|---|---|---|---|---|
| Aluminate sorbents ($LiCl{\cdot}2Al(OH)_3{\cdot}nH_2O$) | LiCl intercalation into gibbsite-like layers; water elution | ~7–8 mg Li/g | High selectivity; mild regeneration; industrial track record | Low capacity; large sorbent inventories | Commercial (Hombre Muerto; Qinghai; Centenario) | Paranthaman et al. (2017); Boroumand and Razmjou (2024) |
| Mn-spinel ion sieves ($H_{1.6}Mn_{1.6}O_4$) | Ion exchange in $Li^+$-sized spinel vacancies; | ~72 mg/g theoretical; 30–40 mg/g realized | Highest capacities and selectivity | Mn dissolution during acid regeneration | Pilot | Chitrakar et al. (2001); Xu et al. (2016) |

| | | | | | | |
|---|---|---|---|---|---|---|
| | acid elution | | | | | |
| Ti ion sieves ($H_2TiO_3$) | Layered ion exchange; acid elution | ~33 mg/g from brine | Better framework stability | Slow elution kinetics | Laboratory / pilot | Chitrakar et al. (2014); Xu et al. (2016) |
| Solvent extraction (TBP–$FeCl_4^-$) | Coordination extraction of LiCl into organic phase | — | Tolerates very high Mg/Li | Solvent losses; corrosion | Limited industrial | Zhou et al. (2012) |
| Nanofiltration / electromembrane | Charge- and size-based $Mg^{2+}/Li^+$ rejection | — | Continuous, modular | Fouling; energy; dilute permeate | Pilot / demonstration | Xu et al. (2021); Vera et al. (2023) |
| Electrochemical intercalation ($LiFePO_4$) | Selective $Li^+$ (de)intercalation between paired electrodes | Electrode-limited | Low theoretical energy; no reagent cycle | Electrode durability; scale-up | Laboratory / pilot | Pasta et al. (2012); Battistel et al. (2020) |

### 3.4 Data-driven design and optimization of extraction

The materials problems of Section 3.3 capacity–stability trade-offs, selectivity under competing-ion loads, degradation over cycling are high-dimensional design problems with expensive experiments, which is the setting in which surrogate modeling pays. Four validated lines of work illustrate the state of the art. First, computational screening seeded the field: density-functional calculations over lithium–metal–oxide phase space identified candidate ion-exchange materials for brine extraction before synthesis, an early demonstration that materials databases could be queried for extraction chemistry rather than battery chemistry alone (Snydacker et al., 2018). The subsequent maturation of universal graph-network interatomic potentials trained on materials databases (Chen and Ong, 2022) and the large-scale expansion of predicted stable crystals (Merchant et al., 2023) has widened that searchable space by orders of magnitude, though these tools have yet to be systematically applied to sorbent discovery.

Second, interpretable machine learning has now closed the loop to synthesis. Zhang et al. (2025) trained models linking dopant identity and synthesis variables to the capacity and cycling stability of aluminum-based sorbents, used feature attribution to extract design rules balancing the two, and synthesized the recommended compositions which delivered roughly 40% higher stable capacity than conventional aluminate sorbents in real brines of several chemistries. This is, to date, the clearest published demonstration in lithium extraction of the design–predict–validate cycle that materials informatics has promised.

Third, gradient-boosting models trained on compiled adsorption literature predict lithium uptake across sorbent families and water chemistries with $R^2 \approx 0.98$, with feature-importance analysis consistently ranking solution conditions above sorbent descriptors a

useful corrective to a literature that reports capacities without standardizing matrices (Xu et al., 2024). In membrane science, random-forest analysis of ion-transport experiments identified electrostatic descriptors as the dominant controls on selectivity in polymeric membranes, mechanistic insight directly relevant to designing Li/Mg-selective nanofiltration (Ritt et al., 2022).

Fourth, classical statistical optimization remains quietly productive at process scale. Response-surface methodology unfashionable but rigorous located the temperature, time, solids-loading, and $CO_2$-flow optimum of a $CO_2$-assisted lithium leach at 97% recovery (Milicevic Neumann et al., 2024), and analogous designs pervade the hydrometallurgical literature. The lesson we draw is that the appropriate tool scales with data availability: designed experiments where runs are few, boosted trees where the literature can be compiled, deep models where databases exist.

What is largely absent from the peer-reviewed record, despite frequent mention in industry material, is the plant-scale layer: model-predictive control of evaporation pond networks, digital twins of DLE trains, autonomous operation of extraction circuits. We found no peer-reviewed demonstrations at time of writing, and we flag this the gap between laboratory surrogate models and operating plants as among the most consequential open problems in the field (Section 7).

## 4. From concentrate to battery grade: separation and purification

The lithium that leaves an extraction circuit is not yet a product. Battery cathode and electrolyte manufacture requires lithium carbonate or hydroxide exceeding 99.5% purity, with the divalent impurities magnesium and calcium controlled to trace levels because they co-precipitate with, and substitute into, cathode precursors (Choe et al., 2024). Purification is where the selectivity problem of Section 1 reappears in its most concentrated form, and its economics are easily underestimated: refining accounts for an estimated 30–40% of total lithium production cost, and magnesium removal alone for the majority of refinery operating cost (Choe et al., 2024).

The standard purification train is sequential precipitation followed by recrystallization. Lime precipitates magnesium as $Mg(OH)_2$ ($K_{sp} \approx 10^{-11}$), soda ash strips calcium as $CaCO_3$, and the polished liquor is carbonated to crude $Li_2CO_3$. Final upgrading exploits the bicarbonate cycle: sparging a carbonate slurry with $CO_2$ converts sparingly soluble $Li_2CO_3$ to soluble $LiHCO_3$, leaving insoluble impurities to be filtered off, after which heating reverses the equilibrium and re-precipitates carbonate of battery grade. Ion-exchange polishing removes residual divalents to final specification (Choe et al., 2024). Lithium hydroxide increasingly demanded for high-nickel cathodes because NMC and NCA lithiation proceeds at lower temperature with LiOH is produced either by causticizing carbonate with lime or, from sulfate liquors, by electrochemical or crystallization routes; on a life-cycle basis hydroxide from brine carries roughly half the emissions of hydroxide from spodumene (Kelly et al., 2021).

Two research directions merit attention. The first is impurity-tolerant cathode synthesis: Choe et al. (2024) make the provocative, quantified argument that relaxing purity specifications where electrochemically justified could reduce refining cost and emissions

substantially a systems-level trade between refinery chemistry and cathode performance that has received far less modeling attention than either endpoint alone. The second is direct production of battery-grade product from DLE eluates, which are cleaner than pond concentrates and may allow shorter purification trains; the quantitative literature here is thin, and process-level data from the operating plants listed in Section 3.3 would be more valuable than another laboratory sorbent study.

## 5. Closing the loop: recycling as the fourth resource

### 5.1 The feedstock and its preparation

Spent lithium-ion batteries are a high-grade, chemically complex ore: cathode black mass carries several percent lithium alongside nickel, cobalt, and manganese at concentrations far above any natural deposit, but embedded in a manufactured architecture of aluminum and copper foils, fluorinated binder, flammable electrolyte, and stored electrical energy (Harper et al., 2019). Recycling flowsheets therefore begin with discharge and stabilization, disassembly to module or cell level, and comminution to black mass under inert or thermal pretreatment, with electrolyte and binder fluorine managed as HF-generating hazards (Neumann et al., 2022; Makuza et al., 2021). The feedstock is also heterogeneous in a way natural ores are not: chemistry varies cell to cell, state of health varies pack to pack, and neither is labeled which is precisely why the sorting and triage problems of Section 5.5 are machine-learning problems.

### 5.2 Pyrometallurgical processing

Smelting shredded cells or modules in a reducing furnace collects nickel, cobalt, and copper into an alloy for downstream refining, tolerating essentially any feed composition. Its chemistry, however, is unkind to lithium: as the most oxophilic of the recoverable metals, lithium reports quantitatively to the slag, from which recovery requires a dedicated hydrometallurgical leach that is rarely economic; in most operating configurations the lithium is simply lost to slag used as construction aggregate (Makuza et al., 2021; Harper et al., 2019). Pyrometallurgy thus sits in tension with lithium-specific recovery mandates (Section 5.6): it is the most robust route to cobalt and nickel and among the worst routes to lithium.

### 5.3 Hydrometallurgical processing

Hydrometallurgical flowsheets leach black mass in acid most commonly 1–2 M $H_2SO_4$ with $H_2O_2$ as reductant, converting insoluble $Co^{3+}/Mn^{4+}$ oxides to soluble divalents routinely dissolving over 95% of the lithium, nickel, cobalt, and manganese at 60–80 °C (Neumann et al., 2022; Biswal et al., 2024). Downstream separation by solvent extraction and precipitation recovers each metal at battery precursor purity. The route's weaknesses are reagent consumption, saline effluents, and the position of lithium at the end of the recovery train: after nickel, cobalt, and manganese are stripped, lithium is precipitated from a liquor accumulated through every upstream step, with cumulative losses at each. Milder lixiviants address the reagent burden: gluconic acid with peroxide leaches >98% of lithium, cobalt, and manganese from NMC black mass under optimized conditions (Lerchbammer et al.,

2023), and citric and other carboxylic acids perform comparably in a large laboratory literature, though techno-economic validation at scale remains sparse (Biswal et al., 2024).

### 5.4 Early-stage and selective lithium recovery

An instructive reversal of the conventional order is to take lithium out first. Carbonated-water leaching converts lithium in thermally pretreated black mass to soluble $LiHCO_3$ the same bicarbonate equilibrium used in purification (Section 4) while nickel, cobalt, and manganese remain in the solid: the COOL process mobilizes up to ~95% of the lithium with water and $CO_2$ alone, leaving a lithium-depleted transition-metal concentrate for conventional processing (Mende et al., 2023), and response-surface optimization of a related $CO_2$-assisted leach reached 97% lithium recovery (Milicevic Neumann et al., 2024). Early-stage lithium recovery is attractive on three counts: it produces lithium before the loss-accumulating separation train, its selectivity is thermodynamically clean, and its mild conditions suit decentralized preprocessing. Its constraint is thermal pretreatment cost and the need to demonstrate battery-grade product at scale.

### 5.5 Direct regeneration, sorting, and data-driven triage

Direct recycling aims higher than elemental recovery: it would restore degraded cathode particles to electrochemical health replenishing lithium, healing defects without ever dissolving the crystal, preserving the embedded value of particle engineering (Gaines et al., 2021). Relithiation by hydrothermal, molten-salt, and solid-state routes has been demonstrated on laboratory and pilot feeds, and cost modeling ranks direct routes as potentially the most profitable where feedstock is homogeneous (Gaines et al., 2021).

That qualifier is the crux, and it converts direct recycling from a chemistry problem into an information problem. Regeneration chemistry is specific to cathode composition and degradation state, but arriving feedstock is unlabeled. Tao et al. (2023) demonstrated a practical answer: federated machine-learning models, trained across organizations without sharing proprietary data, classified retired cells by cathode chemistry from a single standardized charge–discharge cycle with 1–3% error, and the enabled chemistry-specific routing more than doubled the modeled profitability of direct recycling. Upstream of chemistry classification sits health assessment: data-driven models predict remaining cycle life from early-cycle features with better than 10% error (Severson et al., 2019), and health-estimation frameworks for retired EV cells support reuse-versus-recycle triage with capacity-estimation errors below 2% (Cui et al., 2024). At the physical layer, computer-vision systems instance segmentation guiding robotic grasping have been demonstrated for pack-level disassembly of commercial EV batteries, addressing a task whose manual form is hazardous and cost-limiting (Zorn et al., 2022). A recent perspective maps these threads onto the full reuse–recycle–remanufacture pipeline and identifies data scarcity and heterogeneity as the field's central obstacle (Tao et al., 2026) the same diagnosis we reach for extraction in Section 7.

### 5.6 Policy as a chemistry constraint

Regulation now writes chemistry requirements directly. The European Union battery regulation (2023/1542) mandates recycling efficiencies of 65% by mass for lithium-based

batteries by the end of 2025 and 70% by 2030; lithium-specific material recovery of 50% by the end of 2027, rising to 80% by 2031; and minimum recycled content in new batteries including 6% recycled lithium from 2031 that effectively obliges closed-loop flows (European Union, 2023). The 80% lithium-recovery target is chemically pointed: it is unreachable by slag-discarding pyrometallurgy and demanding even for conventional hydrometallurgy with end-of-train lithium recovery, and thus functions as an implicit subsidy for the early-stage and direct routes of Sections 5.4 and 5.5. Table 3 compares the routes against these targets.

**Table 3.** Recycling process routes compared against the lithium-recovery requirements of Regulation (EU) 2023/1542 (50% Li recovery by end-2027; 80% by end-2031).

| Route | Principle | Fate of lithium | Strengths | Limitations | Fit to 80% Li-recovery target |
|---|---|---|---|---|---|
| Pyrometallurgical | Reductive smelting to Ni–Co–Cu alloy | Reports to slag; rarely recovered | Robust to any feed; mature | Li loss; high energy; off-gas management | Poor without dedicated slag treatment |
| Hydrometallurgical | Acid leach ($H_2SO_4/H_2O_2$) then sequential separation | >95% leached; recovered at end of train | Battery-grade products; high recoveries | Reagents; effluent; cumulative losses | Achievable with optimized flowsheets |
| Early-stage selective ($CO_2$–water) | Selective $LiHCO_3$ leach from thermally treated black mass | ~95–97% recovered first | Chemically clean selectivity; mild conditions | Thermal pretreatment; scale unproven | Designed around it |
| Direct regeneration | Relithiation and healing of intact cathode particles | Retained in regenerated cathode | Preserves embedded value; lowest modeled cost | Requires sorted, homogeneous feed | Compatible; depends on ML sorting |
| Bioleaching | Microbially generated lixiviants | High recovery, slow kinetics | Low reagent intensity | Rates; scale-up; consistency | Unproven at scale |

Sources: Makuza et al. (2021); Neumann et al. (2022); Biswal et al. (2024); Mende et al. (2023); Milicevic Neumann et al. (2024); Gaines et al. (2021); Harper et al. (2019); European Union (2023).

## 6. Environmental performance across supply routes

Comparative life-cycle assessment supports three robust conclusions. First, the ore and brine routes differ by roughly an order of magnitude in greenhouse-gas intensity for lithium carbonate about 20.4 t $CO_2$e per tonne via Australian spodumene processed in China against 2.7–3.1 t $CO_2$e via Chilean brine with the gap driven by calcination and acid-roast energy (Kelly et al., 2021). The difference propagates to cell level, where cathode-stage emissions differ by up to tens of percent depending on lithium source (Kelly et al., 2021). Second, the brine route's advantage is not free: it relocates impact from energy to water in some of Earth's driest basins. The hydrological interpretation is genuinely contested isotopic and modeling work in the Salar de Atacama shows that pumped brine and regional freshwater are strongly decoupled and that relic groundwater confounds simple depletion narratives (Moran et al., 2022) but ecological observation is harder to argue with: flamingo abundance in the Lithium Triangle correlates negatively with the combination of mining-related water-level decline and climate stress (Gutiérrez et al., 2022). Third, recycling is environmentally favorable relative to any primary route where collection logistics are sane, with hydrometallurgical and direct routes outperforming pyrometallurgical ones on energy and emissions (Harper et al., 2019; Biswal et al., 2024).

DLE complicates rather than resolves this picture. It shrinks pond footprints and shortens residence times, but adds process energy, fresh-water demand for elution and washing, and reagent cycles whose burdens depend on site-specific brine chemistry; credible assessment requires plant data that operators have been slow to publish (Vera et al., 2023). Our reading of the evidence is that no lithium supply route is categorically clean, and that the useful comparisons are marginal ones which route, at which site, displaces which alternative a framing that the aggregated life-cycle numbers of Fig. 4 support but cannot settle alone.

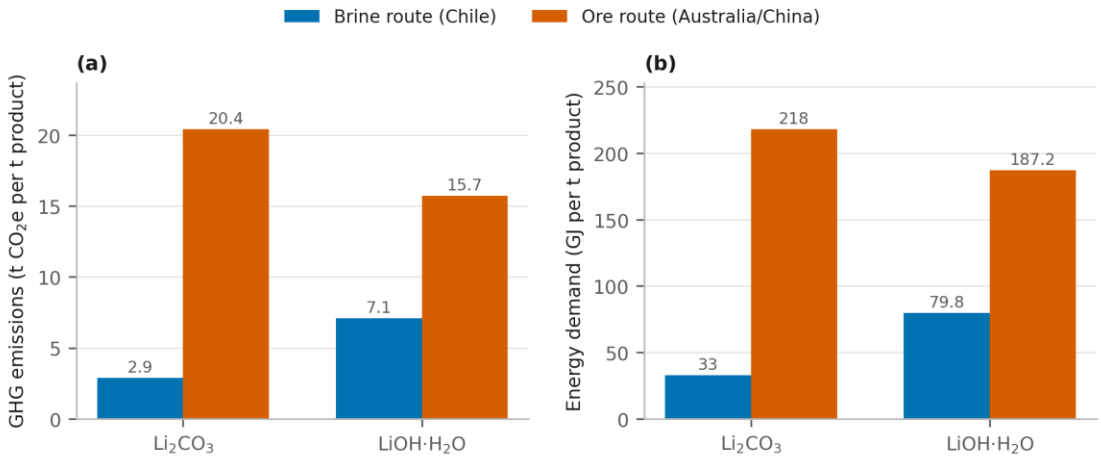


**Fig. 4.** Cradle-to-gate life-cycle comparison of brine (Chilean salar) and ore (Australian spodumene, Chinese conversion) routes to lithium carbonate and lithium hydroxide monohydrate: (a) greenhouse-gas emissions; (b) primary energy demand. Brine-route values are midpoints of the reported ranges (2.7–3.1 t $CO_2$e/t and 6.9–7.3 t $CO_2$e/t; 30–36 GJ/t and 76.6–82.9 GJ/t). Data from Kelly et al. (2021).

## 7. Synthesis: an integrated chemistry–data framework

### 7.1 One selectivity problem, four expressions

Read as a whole, the supply chain reviewed above is a single chemical problem expressed four ways. In exploration, the problem is inferring where selective enrichment already happened, from proxies because lithium itself is spectroscopically silent at a distance. In primary extraction, it is engineering selectivity that nature did not finish thermally in the spodumene route, temporally in the ponds, structurally in DLE materials. In purification, it is the final decrement of the same competition, lithium against magnesium and calcium, now fought over the last few hundred ppm at the highest marginal cost. In recycling, it is selectivity against a manufactured matrix, with the added twist that the feedstock's composition is information someone once had and discarded. This unity is practically consequential: advances transfer. The bicarbonate equilibrium purifies primary carbonate and selectively leaches secondary black mass; aluminate sorbent chemistry developed for salars is deployed on oilfield brines; the Mn-framework stabilization problem of ion sieves is the degradation chemistry of spinel cathodes read in reverse.

### 7.2 Where data-driven methods have earned their place

Table 4 assembles the machine-learning applications reviewed above, with tasks, methods, data scales, and reported performance. Three patterns organize it. First, the successes share a structure: a well-posed prediction target, training data that already existed (legacy brine analyses, compiled adsorption studies, cycling records), and validation against ground truth outside the training set drilled wells, synthesized sorbents, sorted cells. Second, the data scales are modest; these are hundreds-to-thousands-of-samples problems where gradient-boosted trees and random forests remain the honest default, not the million-structure regime of foundation-model materials science (Merchant et al., 2023). Third, the binding constraint everywhere is data, not algorithms: producers hold process histories as proprietary, academic studies report capacities in incomparable matrices, and no public benchmark exists for DLE sorbent performance or recycling feed characterization. The economic stakes of closing this gap are not small; risk-premium modeling puts the financing penalty attached to critical-minerals project uncertainty in the hundreds of billions of dollars, with AI-driven risk reduction identified as a principal lever (Vespignani and Smyth, 2024).

**Table 4.** Validated machine-learning and data-driven applications across the lithium supply chain. All entries are published, peer-reviewed demonstrations; performance figures are as reported by the cited studies.

| Stage | Task | Method | Data | Reported performance | Source |
|---|---|---|---|---|---|
| Resource assessment | Map brine Li and estimate resource, Smackover Fm. | Random forest | Legacy USGS produced-water analyses | 5.1–19 Mt Li in place, southern Arkansas | Knierim et al. (2024) |
| Resource assessment | Predict produced-water Li from major | GBT, XGBoost, | Legacy well analyses, | Accurate prediction; cross- | Attanasi et al. (2024, |

| Stage | Task | Method | Data | Reported performance | Source |
|---|---|---|---|---|---|
| | ions | DNN | multiple basins | basin transfer tests | 2026) |
| Exploration | Pegmatite prospectivity mapping | ANN; SVM on Sentinel-2 | Geology, stream geochemistry, satellite imagery | Known Li mines recovered; false positives suppressed | Köhler et al. (2021); Cardoso-Fernandes et al. (2020a) |
| Grade control | Li quantification and mineral mapping | LIBS calibration models | Crushed pegmatite ore spectra | $R^2 \approx 0.98$ vs. ICP-AES | Rifai et al. (2022) |
| Materials discovery | Screen Li–M–O ion-exchange sorbents | High-throughput DFT | Computed phase stability | Candidate extraction materials identified | Snydacker et al. (2018) |
| Sorbent design | Dope Al-based sorbents for capacity + stability | Interpretable ML with experimental validation | Doped-sorbent synthesis dataset | ~40% higher stable capacity in real brines | Zhang et al. (2025) |
| Process modeling | Predict Li adsorption across water chemistries | XGBoost (16 features) | Compiled adsorption literature | $R^2 \approx 0.98$ | Xu et al. (2024) |
| Membranes | Identify controls on ion selectivity | Random forest on transport data | 126 descriptors, 18 ions | Electrostatic descriptors ≈75% of predictive weight | Ritt et al. (2022) |
| Process optimization | Optimize $CO_2$-assisted Li leach | Response surface methodology | Central-composite designed experiments | 97% Li recovery at optimum | Milicevic Neumann et al. (2024) |
| Recycling | Sort retired cells by cathode chemistry | Federated learning | 130 cells, 5 chemistries, 7 manufacturers | 1–3% sorting error; ≈2.3× direct-recycling profit | Tao et al. (2023) |
| Recycling | Robotic pack disassembly | Instance segmentation + robotics | 30–200 images, augmented | Demonstrated component detection and grasping | Zorn et al. (2022) |
| Reuse triage | Predict cycle life early | Regularized regression | 124-cell open cycling dataset | 9.1% error from first 100 cycles | Severson et al. (2019) |
| Reuse triage | Estimate state of health of retired | Elastic net | 15-month aging campaign, 8 | MAPE 1.4–2.3% | Cui et al. (2024) |

| Stage | Task | Method | Data | Reported performance | Source |
|---|---|---|---|---|---|
| | cells | | retired cells | | |

### 7.3 A framework and its gaps

Fig. 5 sketches the integration we argue for: a loop in which geochemical databases train resource models; resource models target field measurement (LIBS, portable XRF) whose results re-enter the databases; extraction chemistry generates standardized performance data that train sorbent- and process-level surrogates; and plant operation, in turn, produces the time-series data that the missing plant-scale layer control, twins, autonomous optimization would require. Every arrow in that loop exists somewhere in the literature reviewed here except the last, and the asymmetry is telling: the field has learned to predict materials and map resources faster than it has learned to instrument and publish plant behavior. We identify four specific gaps. (1) Standardized reporting: sorbent capacities, selectivities, and cycle lives measured in defined synthetic brines, as battery science standardized rate and cycling protocols. (2) Public benchmarks: a shared DLE dataset and a black-mass characterization dataset would do for this field what open cycling datasets (Severson et al., 2019) did for battery prognostics. (3) Transferability studies: models that survive transport between basins and feedstocks (Attanasi et al., 2026) are worth ten single-site demonstrations. (4) Closing the control loop: peer-reviewed demonstrations of model-based control on operating extraction or recycling circuits, however small.

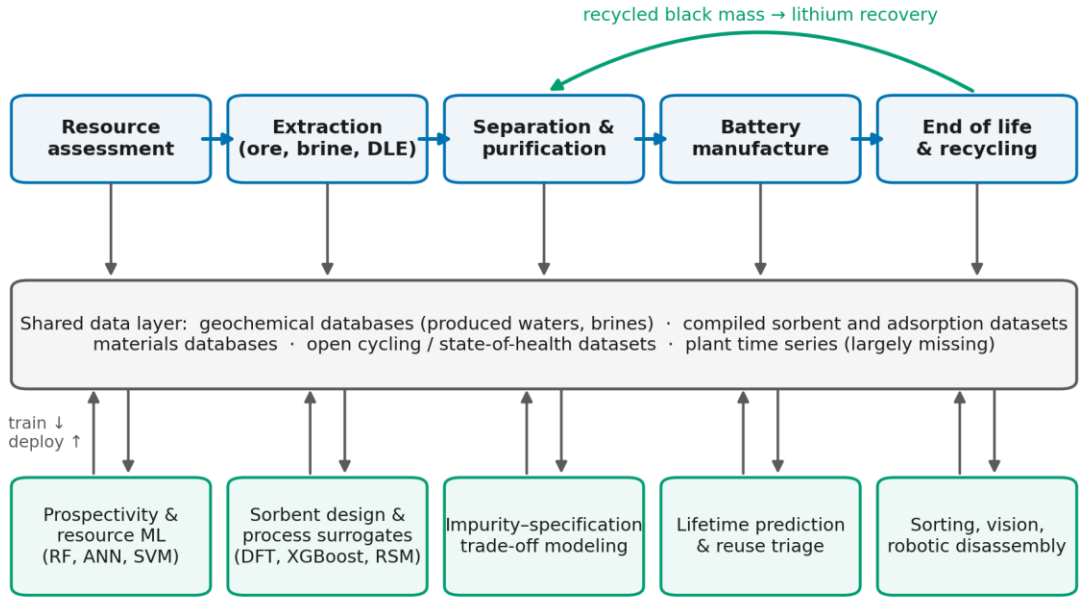


**Fig. 5.** An integrated chemistry–data framework for the lithium supply chain. The chemical value chain (top) exchanges data with a shared data layer (middle) that trains the machine-learning and optimization applications (bottom), which deploy back to their stages. All elements of the loop have published demonstrations (Table 4) except plant-scale time series and control, which remain the principal gap.

## 8. Conclusions

Lithium supply is most often narrated as a race between accelerating demand curves and the slow cadence of mine openings. The view from chemistry, developed throughout this review, is different and, we argue, more useful: the true constraint is selectivity. The history of lithium recovery is, in essence, the history of purchasing selectivity by different currencies with energy in spodumene conversion, with time in evaporation ponds, with engineered materials in direct lithium extraction, and with information in recycling and every data-driven approach that now surrounds the field. Resources themselves are not the limit: identified global inventories have quintupled in only fifteen years, and machine-learning assessment continues to uncover lithium within databases the industry already owned. The genuine bottleneck is the conversion of resource into supply a limit set by process chemistry operating under price volatility that systematically punishes slow, inflexible flowsheets.

From the evidence assembled in this review, three developments demand the field's concentrated attention. First, direct lithium extraction stands as the defining primary technology of this era already industrial in its aluminate form and its remaining barriers lie not in concept but in sorbent lifetime and in site-honest accounting of water and energy demands. Second, early-stage and direct recycling routes constitute the only plausible answer to lithium-recovery mandates that conventional flowsheets are structurally unable to meet; their enabling problems feed identification, state-of-health triage, and disassembly are already yielding to machine learning in published, experimentally validated demonstrations. Third, and cutting across every stage of the value chain, the highest-return investment remains the most unglamorous one: standardized, shared data.

It is worth stating plainly that the machine-learning results that genuinely changed this field a resource assessment that moved a national inventory, a sorbent designed to a model's specification, a sorting system that doubled recycling profit were all built on data that someone deliberately chose to curate and release. The chemistry of lithium recovery is hard, but it is increasingly well understood. The data infrastructure around it is not governed by thermodynamics or kinetics it is governed by choice. It is, therefore, the one part of this challenge the field can simply choose to build faster.

## Credit authorship contribution statement

Mustafa Rezaei: Conceptualization, Methodology, Investigation, Visualization, writing original draft, Writing review & editing, Project administration. Gabriela Sanchez-Lecuona: Investigation, Visualization, Writing original draft, Writing review & editing. Omid Abdolazimi: Investigation, Formal analysis, Writing review & editing.


## Funding

This research did not receive any specific grant from funding agencies in the public, commercial, or not-for-profit sectors.


## Declaration of Competing Interest

The authors declare that they have no known competing financial interests or personal relationships that could have appeared to influence the work reported in this paper.

## Data availability

No new data were created or analyzed in this review. All data discussed are contained in the cited publications and in the public databases and repositories referenced therein.

## Declaration of generative AI and AI-assisted technologies in the manuscript preparation process

During the preparation of this work, the authors used generative AI to improve the fluency and conciseness of the English language, refine sentence structure, and eliminate unnecessary wording. After using this tool/service, the authors reviewed and edited the content as needed and takes full responsibility for the content of the published article.

## References


Attanasi, E.D., Coburn, T.C., Freeman, P.A., 2024. Machine learning approaches to identify lithium concentration in petroleum produced waters. Miner. Econ. 37, 477–497. https://doi.org/10.1007/s13563-023-00409-8

Attanasi, E.D., McDevitt, B., Freeman, P.A., Coburn, T.C., 2026. Evaluating machine learning approaches to identify and predict oil and gas produced water lithium concentrations. Data Sci. Sci. 5, 2624195. https://doi.org/10.1080/26941899.2026.2624195

Battistel, A., Palagonia, M.S., Brogioli, D., La Mantia, F., Trócoli, R., 2020. Electrochemical methods for lithium recovery: a comprehensive and critical review. Adv. Mater. 32, 1905440. https://doi.org/10.1002/adma.201905440

Benson, T.R., Coble, M.A., Dilles, J.H., 2023. Hydrothermal enrichment of lithium in intracalderaillite-bearing claystones. Sci. Adv. 9, eadh8183. https://doi.org/10.1126/sciadv.adh8183

Biswal, B.K., Zhang, B., Tran, P.T.M., Zhang, J., Balasubramanian, R., 2024. Recycling of spent lithium-ion batteries for a sustainable future: recent advancements. Chem. Soc. Rev. 53, 5552–5592. https://doi.org/10.1039/D3CS00898C

Boroumand, Y., Razmjou, A., 2024. Adsorption-type aluminium-based direct lithium extraction: the effect of heat, salinity and lithium content. Desalination 577, 117406. https://doi.org/10.1016/j.desal.2024.117406

Bowell, R.J., Lagos, L., de los Hoyos, C.R., Declercq, J., 2020. Classification and characteristics of natural lithium resources. Elements 16, 259–264. https://doi.org/10.2138/gselements.16.4.259

Bradley, D.C., McCauley, A.D., Stillings, L.M., 2017. Mineral-Deposit Model for Lithium-Cesium-Tantalum Pegmatites. U.S. Geological Survey Scientific Investigations Report 2010-5070-O. https://doi.org/10.3133/sir20105070O

Cardoso-Fernandes, J., Teodoro, A.C., Lima, A., Roda-Robles, E., 2020a. Semi-automatization of support vector machines to map lithium (Li) bearing pegmatites. Remote Sens. 12, 2319. https://doi.org/10.3390/rs12142319

Cardoso-Fernandes, J., Teodoro, A.C., Lima, A., Perrotta, M., Roda-Robles, E., 2020b. Detecting lithium (Li) mineralizations from space: current research and future perspectives. Appl. Sci. 10, 1785. https://doi.org/10.3390/app10051785

Castor, S.B., Henry, C.D., 2020. Lithium-rich claystone in the McDermitt caldera, Nevada, USA: geologic, mineralogical, and geochemical characteristics and possible origin. Minerals 10, 68. https://doi.org/10.3390/min10010068

Chen, C., Ong, S.P., 2022. A universal graph deep learning interatomic potential for the periodic table. Nat. Comput. Sci. 2, 718–728. https://doi.org/10.1038/s43588-022-00349-3

Chitrakar, R., Kanoh, H., Miyai, Y., Ooi, K., 2001. Recovery of lithium from seawater using manganese oxide adsorbent (H1.6Mn1.6O4) derived from Li1.6Mn1.6O4. Ind. Eng. Chem. Res. 40, 2054–2058. https://doi.org/10.1021/ie000911h

Chitrakar, R., Makita, Y., Ooi, K., Sonoda, A., 2014. Lithium recovery from salt lake brine by H2TiO3. Dalton Trans. 43, 8933–8939. https://doi.org/10.1039/C4DT00467A

Choe, G., Kim, H., Kwon, J., Jung, W., Park, K.-Y., Kim, Y.-T., 2024. Re-evaluation of battery-grade lithium purity toward sustainable batteries. Nat. Commun. 15, 1185. https://doi.org/10.1038/s41467-024-44812-3

Choubey, P.K., Kim, M.-S., Srivastava, R.R., Lee, J.-C., Lee, J.-Y., 2016. Advance review on the exploitation of the prominent energy-storage element: lithium. Part I: From mineral and brine resources. Miner. Eng. 89, 119–137. https://doi.org/10.1016/j.mineng.2016.01.010

Cui, X., Khan, M.A., Pozzato, G., Singh, S., Sharma, R., Onori, S., 2024. Taking second-life batteries from exhausted to empowered using experiments, data analysis, and health estimation. Cell Rep. Phys. Sci. 5, 101941. https://doi.org/10.1016/j.xcrp.2024.101941

Dessemond, C., Lajoie-Leroux, F., Soucy, G., Laroche, N., Magnan, J.-F., 2019. Spodumene: the lithium market, resources and processes. Minerals 9, 334. https://doi.org/10.3390/min9060334

Dugamin, E.J.M., Richard, A., Cathelineau, M., Boiron, M.-C., Despinois, F., Brisset, A., 2021. Groundwater in sedimentary basins as potential lithium resource: a global prospective study. Sci. Rep. 11, 21091. https://doi.org/10.1038/s41598-021-99912-7

Emproto, C., Benson, T.R., Gagnon, C.A., Baek, W., Ibarra, D.E., Simon, A.C., 2025. Clay chemistry of the Thacker Pass deposit, Nevada: implications for the formation of high-

grade volcano-sedimentary lithium resources. Econ. Geol. 120, 1047–1070. https://doi.org/10.5382/econgeo.5155

Eramet, 2024. Eramet inaugurates Centenario, its first direct lithium extraction plant in Argentina. Press release, 3 July 2024. https://www.eramet.com (accessed 6 August 2026).

European Union, 2023. Regulation (EU) 2023/1542 of the European Parliament and of the Council of 12 July 2023 concerning batteries and waste batteries. Off. J. Eur. Union L 191, 1–117.

Flexer, V., Baspineiro, C.F., Galli, C.I., 2018. Lithium recovery from brines: a vital raw material for green energies with a potential environmental impact in its mining and processing. Sci. Total Environ.639,1188–1204. https://doi.org/10.1016/j.scitotenv.2018.05.223

Gaines, L., Dai, Q., Vaughey, J.T., Gillard, S., 2021. Direct recycling R&D at the ReCell Center. Recycling 6, 31. https://doi.org/10.3390/recycling6020031

Gutiérrez, J.S., Moore, J.N., Donnelly, J.P., Dorador, C., Navedo, J.G., Senner, N.R., 2022. Climate change and lithium mining influence flamingo abundance in the Lithium Triangle. Proc. R. Soc. B 289, 20212388. https://doi.org/10.1098/rspb.2021.2388

Harmon, R.S., Lu, P.L., Curry, A.C., Murray, R.M., Richter, D.D., 2025. LIBS as a tool for Li-pegmatite exploration and prospect evaluation: soil mica and soil analysis from the Carolina Tin-Spodumene Belt. Appl. Geochem. 191, 106534. https://doi.org/10.1016/j.apgeochem.2025.106534

Harper, G., Sommerville, R., Kendrick, E., Driscoll, L., Slater, P., Stolkin, R., et al., 2019. Recycling lithium-ion batteries from electric vehicles. Nature 575, 75–86. https://doi.org/10.1038/s41586-019-1682-5

IEA, 2025. Global Critical Minerals Outlook 2025. International Energy Agency, Paris. https://www.iea.org/reports/global-critical-minerals-outlook-2025

Karrech, A., Azadi, M.R., Elchalakani, M., Shahin, M.A., Seibi, A.C., 2020. A review on methods for liberating lithium from pegmatites. Miner. Eng. 145, 106085. https://doi.org/10.1016/j.mineng.2019.106085

Kelly, J.C., Wang, M., Dai, Q., Winjobi, O., 2021. Energy, greenhouse gas, and water life cycle analysis of lithium carbonate and lithium hydroxide monohydrate from brine and ore resources and their use in lithium ion battery cathodes and lithium ion batteries. Resour. Conserv. Recycl. 174, 105762. https://doi.org/10.1016/j.resconrec.2021.105762

Kesler, S.E., Gruber, P.W., Medina, P.A., Keoleian, G.A., Everson, M.P., Wallington, T.J., 2012. Global lithium resources: relative importance of pegmatite, brine and other deposits. Ore Geol. Rev. 48, 55–69. https://doi.org/10.1016/j.oregeorev.2012.05.006

Knierim, K.J., Blondes, M.S., Masterson, A.L., Freeman, P.A., McDevitt, B., Herzberg, A.S., et al., 2024. Evaluation of the lithium resource in the Smackover Formation brines of southern Arkansas using machine learning. Sci. Adv. 10, eadp8149. https://doi.org/10.1126/sciadv.adp8149

Köhler, M., Hanelli, D., Schaefer, S., Barth, A., Knobloch, A., Hielscher, P., Cardoso-Fernandes, J., Lima, A., Teodoro, A.C., 2021. Lithium potential mapping using artificial neural networks: a case study from Central Portugal. Minerals 11, 1046. https://doi.org/10.3390/min11101046

Lawley, C.J.M., McCafferty, A.E., Graham, G.E., Huston, D.L., Kelley, K.D., Czarnota, K., et al., 2022. Data-driven prospectivity modelling of sediment-hosted Zn–Pb mineral systems and their critical raw materials. Ore Geol. Rev. 141, 104635. https://doi.org/10.1016/j.oregeorev.2021.104635

Lerchbammer, R., Gerold, E., Antrekowitsch, H., 2023. Gluconic acid leaching of spent lithium-ion batteries as an environmentally friendly approach to achieve high leaching efficiencies in the recycling of NMC active material. Metals 13, 1330. https://doi.org/10.3390/met13081330

López Steinmetz, R.L., Salvi, S., 2021. Brine grades in Andean salars: when basin size matters. A review of the Lithium Triangle. Earth-Sci. Rev. 217, 103615. https://doi.org/10.1016/j.earscirev.2021.103615

Makuza, B., Tian, Q., Guo, X., Chattopadhyay, K., Yu, D., 2021. Pyrometallurgical options for recycling spent lithium-ion batteries: a comprehensive review. J. Power Sources 491, 229622. https://doi.org/10.1016/j.jpowsour.2021.229622

Mende, R., Kaiser, D., Pavón, S., Bertau, M., 2023. The COOL-process: a holistic approach towards lithium recycling. Waste Biomass Valorization 14, 3027–3042. https://doi.org/10.1007/s12649-023-02043-5

Merchant, A., Batzner, S., Schoenholz, S.S., Aykol, M., Cheon, G., Cubuk, E.D., 2023. Scaling deep learning for materials discovery. Nature 624, 80–85. https://doi.org/10.1038/s41586-023-06735-9

Meshram, P., Pandey, B.D., Mankhand, T.R., 2014. Extraction of lithium from primary and secondary sources by pre-treatment, leaching and separation: a comprehensive review. Hydrometallurgy 150, 192–208. https://doi.org/10.1016/j.hydromet.2014.10.012

Milicevic Neumann, K., Ans, M., Friedrich, B., 2024. Early-stage recovery of lithium from spent batteries via CO2-assisted leaching optimized by response surface methodology. Sci. Rep. 14, 17369. https://doi.org/10.1038/s41598-024-67761-9

Moran, B.J., Boutt, D.F., McKnight, S.V., Jenckes, J., Munk, L.A., Corkran, D., Kirshen, A., 2022. Relic groundwater and prolonged drought confound interpretations of water sustainability and lithium extraction in arid lands. Earth's Future 10, e2021EF002555. https://doi.org/10.1029/2021EF002555

Munk, L.A., Hynek, S.A., Bradley, D.C., Boutt, D., Labay, K., Jochens, H., 2016. Lithium brines: a global perspective. Rev. Econ. Geol. 18, 339–365.

Neumann, J., Petranikova, M., Meeus, M., Gamarra, J.D., Younesi, R., Winter, M., Nowak, S., 2022. Recycling of lithium-ion batteries — current state of the art, circular economy, and next generation recycling. Adv. Energy Mater. 12, 2102917. https://doi.org/10.1002/aenm.202102917

Paranthaman, M.P., Li, L., Luo, J., Hoke, T.C., Ucar, H., Moyer, B.A., Harrison, S., 2017. Recovery of lithium from geothermal brine with lithium–aluminum layered double hydroxide chloride sorbents. Environ. Sci. Technol. 51, 13481–13486. https://doi.org/10.1021/acs.est.7b03464

Pasta, M., Battistel, A., La Mantia, F., 2012. Batteries for lithium recovery from brines. Energy Environ. Sci. 5, 9487–9491. https://doi.org/10.1039/C2EE22977C

Rezaei, M., Sanchez-Lecuona, G., Abdolazimi, O., 2025. A cross-disciplinary review of rare earth elements: deposit types, mineralogy, machine learning, environmental impact, and recycling. Minerals 15, 720. https://doi.org/10.3390/min15070720

Rifai, K., Constantin, M., Yilmaz, A., Özcan, L.Ç., Doucet, F.R., Azami, N., 2022. Quantification of lithium and mineralogical mapping in crushed ore samples using laser induced breakdown spectroscopy. Minerals 12, 253. https://doi.org/10.3390/min12020253

Ritt, C.L., Liu, M., Pham, T.A., Epsztein, R., Kulik, H.J., Elimelech, M., 2022. Machine learning reveals key ion selectivity mechanisms in polymeric membranes. Sci. Adv. 8, eabl5771. https://doi.org/10.1126/sciadv.abl5771

Rudnick, R.L., Gao, S., 2003. Composition of the continental crust. In: Holland, H.D., Turekian, K.K. (Eds.), Treatise on Geochemistry, vol. 3. Elsevier-Pergamon, Oxford, pp. 1–64.

Salakjani, N.K., Singh, P., Nikoloski, A.N., 2016. Mineralogical transformations of spodumene concentrate from Greenbushes, Western Australia. Part 1: Conventional heating. Miner. Eng. 98, 71–79. https://doi.org/10.1016/j.mineng.2016.07.018

Salakjani, N.K., Singh, P., Nikoloski, A.N., 2020. Production of lithium — a literature review. Part 1: Pretreatment of spodumene. Miner. Process. Extr. Metall. Rev. 41, 335–348. https://doi.org/10.1080/08827508.2019.1643343

Sanjuan, B., Gourcerol, B., Millot, R., Rettenmaier, D., Jeandel, E., Rombaut, A., 2022. Lithium-rich geothermal brines in Europe: an update about geochemical characteristics and implications for potential Li resources. Geothermics 101, 102385. https://doi.org/10.1016/j.geothermics.2022.102385

Severson, K.A., Attia, P.M., Jin, N., Perkins, N., Jiang, B., Yang, Z., et al., 2019. Data-driven prediction of battery cycle life before capacity degradation. Nat. Energy 4, 383–391. https://doi.org/10.1038/s41560-019-0356-8

Snydacker, D.H., Hegde, V.I., Aykol, M., Wolverton, C., 2018. Computational discovery of Li–M–O ion exchange materials for lithium extraction from brines. Chem. Mater. 30, 6961–6968. https://doi.org/10.1021/acs.chemmater.7b03509

Stanley, C.J., Jones, G.C., Rumsey, M.S., Blake, C., Roberts, A.C., Stirling, J.A.R., et al., 2007. Jadarite, LiNaSiB3O7(OH), a new mineral species from the Jadar Basin, Serbia. Eur. J. Mineral. 19, 575–580. https://doi.org/10.1127/0935-1221/2007/0019-1741

Stringfellow, W.T., Dobson, P.F., 2021. Technology for the recovery of lithium from geothermal brines. Energies 14, 6805. https://doi.org/10.3390/en14206805

Tabelin, C.B., Dallas, J., Casanova, S., Pelech, T., Bournival, G., Saydam, S., Canbulat, I., 2021. Towards a low-carbon society: a review of lithium resource availability, challenges and innovations in mining, extraction and recycling, and future perspectives. Miner. Eng. 163, 106743. https://doi.org/10.1016/j.mineng.2020.106743

Tao, S., Liu, H., Sun, C., Ji, H., Ji, G., Han, Z., et al., 2023. Collaborative and privacy-preserving retired battery sorting for profitable direct recycling via federated machine learning. Nat. Commun. 14, 8032. https://doi.org/10.1038/s41467-023-43883-y

Tao, S., Moura, S., Brandell, D., Han, Z., Zou, C., Zhang, X., et al., 2026. Artificial intelligence for battery reuse, recycling and remanufacturing. Nat. Rev. Clean Technol. 2, 366–381. https://doi.org/10.1038/s44359-026-00167-0

Teng, F.-Z., McDonough, W.F., Rudnick, R.L., Dalpé, C., Tomascak, P.B., Chappell, B.W., Gao, S., 2004. Lithium isotopic composition and concentration of the upper continental crust. Geochim. Cosmochim. Acta 68, 4167–4178. https://doi.org/10.1016/j.gca.2004.03.031

USGS, 2026. Mineral Commodity Summaries 2026: Lithium. U.S. Geological Survey, Reston, VA. https://doi.org/10.3133/mcs2026

Vera, M.L., Torres, W.R., Galli, C.I., Chagnes, A., Flexer, V., 2023. Environmental impact of direct lithium extraction from brines. Nat. Rev. Earth Environ. 4, 149–165. https://doi.org/10.1038/s43017-022-00387-5

Vespignani, J., Smyth, R., 2024. Artificial intelligence investments reduce risks to critical mineral supply. Nat. Commun. 15, 7304. https://doi.org/10.1038/s41467-024-51661-7

Warren, I., 2021. Techno-Economic Analysis of Lithium Extraction from Geothermal Brines. Report NREL/TP-5700-79178. National Renewable Energy Laboratory, Golden, CO. https://www.nrel.gov/docs/fy21osti/79178.pdf

Xu, P., Hong, J., Qian, X., Xu, Z., Xia, H., Tao, X., Xu, Z., Ni, Q.-Q., 2021. Materials for lithium recovery from salt lake brine. J. Mater. Sci. 56, 16–63. https://doi.org/10.1007/s10853-020-05019-1

Xu, X., Chen, Y., Wan, P., Gasem, K., Wang, K., He, T., Adidharma, H., Fan, M., 2016. Extraction of lithium with functionalized lithium ion-sieves. Prog. Mater. Sci. 84, 276–313. https://doi.org/10.1016/j.pmatsci.2016.09.004

Xu, Z., Ding, Y., Han, S.C., Zhang, C., 2024. Predicting the performance of lithium adsorption and recovery from unconventional water sources with machine learning. Water Res. 266, 122374. https://doi.org/10.1016/j.watres.2024.122374

Zhang, R., Liu, S., Lian, C., Yu, J., Lin, S., 2025. Machine learning-accelerated design of high-efficient lithium adsorbents for salt lake brines. Angew. Chem. Int. Ed. 64, e202503644. https://doi.org/10.1002/anie.202503644

Zhou, Z., Qin, W., Fei, W., 2012. Extraction equilibria of lithium with tributyl phosphate in kerosene and FeCl3. J. Chem. Eng. Data 57, 82–86. https://doi.org/10.1021/je200803h

Zorn, M., Ionescu, C., Klohs, D., Zähl, K., Kisseler, N., Daldrup, A., et al., 2022. An approach for automated disassembly of lithium-ion battery packs and high-quality recycling using computer vision, labeling, and material characterization. Recycling 7, 48. https://doi.org/10.3390/recycling7040048